Biophysical Journal Volume 105 December 2013 2517–2527

Agonist Leukadherin-1 Increases CD11b/CD18-Dependent Adhesion Via Membrane Tethers

Emrah Celik,[†] Mohd. Hafeez Faridi,[‡] Vinay Kumar,[§] Shashank Deep,[§] Vincent T. Moy,[†*] and Vineet Gupta[‡*]
[†]Department of Physiology and Biophysics, University of Miami Miller School of Medicine, Miami, Florida; [‡]Department of Internal Medicine, Rush University Medical Center, Chicago, Illinois; and [§]Department of Chemistry, Indian Institute of Technology, New Delhi, India

ABSTRACT Integrin CD11b/CD18 is a key adhesion receptor that mediates leukocyte migration and immune functions. Leukadherin-1 (LA1) is a small molecule agonist that enhances CD11b/CD18-dependent cell adhesion to its ligand ICAM-1. Here, we used single-molecule force spectroscopy to investigate the biophysical mechanism by which LA1-activated CD11b/CD18 mediates leukocyte adhesion. Between the two distinct populations of CD11b/CD18:ICAM-1 complex that participate in cell adhesion, the cytoskeleton(CSK)-anchored elastic elements and the membrane tethers, we found that LA1 enhanced binding of CD11b/CD18 on K562 cells to ICAM-1 via the formation of long membrane tethers, whereas Mn^{2+} additionally increased ICAM-1 binding via CSK-anchored bonds. LA1 activated wild-type and LFA1$^{-/-}$ neutrophils also showed longer detachment distances and time from ICAM-1-coated atomic force microscopy tips, but significantly lower detachment force, as compared to the Mn^{2+}-activated cells, confirming that LA1 primarily increased membrane-tether bonds to enhance CD11b/CD18:ICAM-1 binding, whereas Mn^{2+} induced additional CSK-anchored bond formation. The results suggest that the two types of agonists differentially activate integrins and couple them to the cellular machinery, providing what we feel are new insights into signal mechanotransduction by such agents.

INTRODUCTION

Adhesion to neighboring cells, extracellular matrix, and ligands is fundamental to a majority of biological cells. Modulation of the process of cell adhesion regulates a variety of functions of these cells and is mediated by an array of cell adhesion receptors that are expressed on cell surfaces. Integrins are a family of $\alpha\beta$ heterodimeric type I adhesion receptors that are present in all mammalian cells and mediate diverse cellular functions. Among them, the $\beta2$ family of integrins is primarily expressed on the surface of leukocytes and consists of four members that share a common β-chain (CD18) and distinct α-chains (CD111a, CD11b, CD11c, and CD11d). The $\beta2$ integrin CD11b/CD18 (also known as Mac-1, $\alpha M\beta2$, and CR3) is expressed primarily in the cells of the innate immune system (including neutrophils, macrophages, and dendritic cells) (1–3). ICAM-1 (CD54) is a member of the immunoglobulin family that is expressed on the surface of vascular endothelial cells and is significantly upregulated upon an inflammatory stimulus (4), where it mediates migration and tissue recruitment of leukocytes from circulation. Leukocyte emigration is a multistep process that includes the steps of cell tethering, slow rolling, firm adhesion, crawling, and transmigration across the endothelial cell barrier (5). Leukocyte rolling along the walls of microvessels involves a generation of thin, long membrane tethers that are not linked to the leukocytic cytoskeleton and that stabilize leukocyte rolling (6,7). Integrin CD11b/CD18, among its various functions, mediates leukocyte emigration from circulation to the inflamed tissue by binding to ICAM-1 (8–10), one of its >30 physiologic ligands, making it an important therapeutic molecular target for reducing the influx of inflammatory leukocytes into tissues and, thus, for the development of antiinflammatory drugs (11). Indeed, studies over the years have targeted $\beta2$ integrins on leukocytes, as well as their ligand ICAM-1, with antagonists that block adhesion of leukocytes to endothelial cell surfaces (12–15). However, a majority of such adhesion blocking agents failed in various human clinical trials (16–19), suggesting a need for alternative ways to reduce leukocyte binding and recruitment into tissues as a way to affect inflammation. We recently described novel small molecule allosteric agonists of CD11b/CD18 (termed leukadherins) that enhance, rather than inhibit, CD11b/CD18-dependent cell adhesion (20). Leukadherin-mediated increase in cell adhesion significantly reduces leukocyte cell migration in vitro and in vivo. It also significantly reduces tissue influx of leukocytes and led to amelioration of inflammatory injury in multiple experimental models (20). This suggests that integrin activation via allosteric agonists (i.e., a type of agonists that modulate the structure and activity of a protein (integrin) by binding to a site distal from the site of activity or ligand binding) may represent, to our knowledge, a novel and effective approach for reducing leukocyte emigration and tissue recruitment and for the development of next generation antiinflammatory therapeutic agents.

However, not all integrin agonists behave in the same way. We recently found that CD11b/CD18 activation with many other agonists, such as the known agonist Mn^{2+} ions or the CD11b activating antibodies, induces

Submitted July 8, 2013, and accepted for publication October 18, 2013.
*Correspondence: vmoy@miami.edu or vineet_gupta@rush.edu
Emrah Celik and Mohd. H. Faridi contributed equally to this work.
Editor: Simon Scheuring.

0006-3495/13/12/2517/11 $2.00
http://dx.doi.org/10.1016/j.bpj.2013.10.020

outside-in signaling in cells, whereas Leukadherin 1 (LA1) does not (21), suggesting that there may be differences in the way different agonists activate and transmit signal from the integrin extracellular domains to the cytoplasm. Our previous data also suggest that, because binding of different types of agonists to the extracellular domains of integrins produces different intracellular signaling outputs and because the extracellular domains are linked to the intracellular signaling machinery via the cytoskeleton, integrin activation with different types of agonists may couple them differently to the cytoskeletal protein machinery. Published data with some ligand-mimetic integrin antagonists also show binding mediated integrin activation (thus, suggesting that these agents function as agonists) and produces outside-in signaling in cells, leading to serious side effects (22–25), supporting our hypothesis. We reasoned that, because integrins couple to cellular cytoskeleton to transduce mechanosignals, understanding the biophysical nature of forces generated upon integrin activation with various agonists would provide useful insights into how different integrin agonists regulate intracellular signaling and cell function.

Atomic force microscopy (AFM)-based single-cell force spectroscopy (SCFS) can be used to quantitatively study cell adhesion to extracellular matrix ligands (26). Here, we used such AFM-based SCFS measurements to quantitatively determine the differences in coupling of CD11b/CD18 to the cytoskeletal machinery when activated with a known agonist (Mn^{2+}) versus the novel, to our knowledge, agonist LA1. We also quantified the agonist-induced changes in adhesive strength of CD11b/CD18 expressing cells and used that information to develop a mechanism of how different integrin agonists may differentially regulate cellular behavior. We found that Mn^{2+} increased cell adhesion primarily via cytoskeleton-anchored integrin bonds, whereas LA1 primarily increased the occurrence of membrane-tethered bonds, suggesting that the two types of agonists may differentially mediate the increase in cellular adhesivity via integrins. Such knowledge should be helpful in designing new integrin agonists in the future.

MATERIALS AND METHODS

Reagents and antibodies

ICAM-1/Fc chimera (referred to as ICAM-1 hereafter) was purchased from R&D Systems (Minneapolis, MN). Fluorescent cell surface labeling reagent BacMam 2.0 CellLight Plasma Membrane-GFP was obtained from Life Technologies (Carlsbad, CA). Highbind 384-well plates were obtained from Corning (Corning, NY). Nonfat milk was obtained from Bio-Rad. All cell culture reagents were purchased from Life Technologies and Mediatech. Fetal bovine serum (FBS) was purchased from Atlanta Biologicals. The antibiotic G418 was purchased from Invivogen and the chemical reagents were obtained from Fluka. For all experimental assays, a stock solution of agonist LA1 (20) was prepared by dissolving the compound in dimethylsulfoxide (DMSO) at a concentration of 10 mM. LA1 was used at a final concentration of 15 μM in the assays by diluting in the assay buffer. The final concentration of DMSO in the assay was ~1%. To control for any DMSO-related effects, DMSO was also included in non-LA1 experiments and was maintained at 1% in all assay buffers.

Animals

Wild-type (WT) C57BL/6J mice (B6) and the B6 CD11a$^{-/-}$ (LFA-1$^{-/-}$, Jax 5257) (27) animals were purchased from the Jackson Laboratories. Animal care and procedures were approved by the Institutional Animal Care and Use Committee (IACUC) and were performed in accordance with institutional guidelines.

Cells and cell lines

K562 cells (ATCC) stably transfected with plasmid encoding WT CD11b/CD18 (K562 CD11b/CD18 cells) have been described previously (28,29) and were maintained in Iscove's modified Dulbecco's medium (IMDM) supplemented with 10% FBS and G418 (0.5 mg/ml).

Cell adhesion assays

Cell adhesion assays using K562 CD11b/CD18 cells or with WT or LFA$^{-/-}$ neutrophils were performed as previously described (20,30) and used immobilized ICAM-1 as the ligand of CD11b/CD18. Briefly, 384-well microtiter plates (Corning) were coated with ICAM-1 (0.35 μg/mL) in phosphate buffered saline (PBS), pH 7.4 containing 1 mM each of Ca^{2+} and Mg^{2+} ions (PBS^{2+} buffer) by incubating overnight at 4°C. The nonspecific sites were subsequently blocked with 1% nonfat milk in Tris buffered saline (TBS), pH 7.4, for 1 h at room temperature before the K562 cell adhesion assay, or with TBS containing 1% gelatin before the neutrophil cell adhesion assay. For the adhesion assay, 30,000 cells were added to each well. For the K562 cell-based assays, cells were suspended in Tris Buffered Saline (TBS), pH 8 containing 1 mM each of Ca^{2+} and Mg^{2+} ions (TBS^{2+} buffer) and incubated in the presence of various agents in the ligand-coated wells of the microtiter plate for 30 min at 37°C. For the neutrophil adhesion assays, neutrophils from 8- to 10-week old WT B6 and LFA-1$^{-/-}$ mice were isolated from thioglycollate-stimulated peritonea according to literature protocols (20). Neutrophils were suspended in serum free medium (IMDM) and incubated with leukadherins in the ligand-coated wells for 10 min at 37°C. The assay plates with either cell type were then gently inverted and kept in the inverted position for 30 min at room temperature to dislodge the nonadherent cells. The remaining adherent cells were fixed using 4% formaldehyde and quantified by imaging microscopy as previously described (20). As previously described (28,30), the input cell number for these imaging-based analyses was calculated by counting the cells adherent in the uncoated microtiter plate wells (which nonspecifically binds almost all input cells) and was used to normalize the data. Assays were performed in triplicate wells. Data reported are from one of at least three independent experiments.

Chemotaxis assay and time-lapse video microscopy

Neutrophil chemotaxis on planar surfaces was performed using Zigmond chambers (Neuro Probe) on acid-cleaned or ICAM-1-coated glass coverslips, according to the protocol described previously (31,32). Briefly, neutrophils were preincubated on a glass coverslip in a humidified chamber in the cell culture media (RPMI 1640 containing 1% FBS) in the presence of agonists Mn^{2+} ions (0.1–1 mM) or LA1 (15 μM), for 5–10 min and the coverslip was then placed on top of Zigmond chambers. A formyl-Met-Leu-Phe (fMLP) (Sigma, F3506) gradient was created in between the Zigmond chambers by placing the assay buffer in one well of the chamber and fMLP (10 μM) containing assay buffer (RPMI 1640 containing 1% FBS) in the other well. The migration of WT or LFA1$^{-/-}$ neutrophils toward fMLP

was recorded at 5- to 30-s intervals for a period of 25 min using either a Nikon Eclipse 90i microscope or a Leica DMI16000 deconvolution microscope, as previously described (20). Images with the Nikon microscope were acquired using a Nikon DS camera with a PLAN APO 20× differential interference contrast microscopy objective and was acquired using the Nikon Imaging software. Leica differential interference contrast images were acquired using an HCX PL APO 40×/0.75 NA objective and a DCF360FX camera driven by LAS-AF software. The neutrophil migration data were analyzed using ImageJ software (NIH) with manual cell tracking using the chemotaxis and migration tool plugins (Ibidi) for ImageJ. Data from 75 to 100 neutrophils were quantified under each condition and from at least three independent experiments.

AFM force measurements

AFM was used to control the relative position of the interacting molecules via expansion or contraction of the 90 μm closed loop piezoelectric translator (P-841.60; Physik Instrumente, Waldbronn, Germany). Sharp cantilevers were used for a single set of ~100 measurements and all the measurements were carried out at 25°C. Force measurements were carried out on a custom-built AFM (33) using Si3N4 cantilevers with a nominal spring constant of 0.02 N/m (MLCT-AUHW; Veeco Probes, Santa Barbara, CA). To prepare the ICAM-1 functionalized AFM cantilevers, ultraviolet-irradiated cantilevers were silanized with 3-aminopropyltriethoxysilane solution in ethanol for 10 min. After incubation of the cantilevers with 0.1% glutaraldehyde for 30 min, they were washed in PBS and incubated with ICAM-1 (2.5 mg/mL) for 45 min at room temperature. The cantilevers were then washed with PBS to remove unbound ICAM-1 and incubated with 1% bovine serum albumin for 45 min to block nonspecific adhesion sites. Typically, cantilevers were functionalized with ICAM-1 on the day of measurements and 3–5 different cantilevers were used for each test condition. To obtain consistent results over many days and given that the cantilevers prepared in different preparation batches could have different ligand densities, the AFM cantilevers prepared in the same batch were used to obtain data from different experimental conditions. Cantilevers were individually calibrated by thermal fluctuation analysis according to the method of Hutter and Bechhoefer (26). The force acting between the molecules was derived from the deflection of the AFM cantilever, which was monitored by reflecting a focused laser beam off the back of the cantilever into a 2-segment photodiode. After calibration, cells were deposited on the petri dish (Falcon 351008) coated with poly-L-lysine (0.1 mg/mL, 16 h incubation at 4°C) and allowed to immobilize for 5 min. The AFM measurement buffer consisted of TBS (10 mM) with 0.1% bovine serum albumin, and 1% DMSO and the various agonists were added to the medium before each assay. A typical force measurement began with lowering the cantilever onto the substrate where adhesive interaction took place between the cell and the functionalized tip. After a specified interaction time, the cantilever was subsequently retracted until complete detachment from the cell surface occurred. A total of 25 force-distance (F-z) curves were acquired for each experimental condition by lowering the tip onto the cell at the rate of 3.75 μm/s, maintaining contact for 2 s, and subsequently retracting the cantilever at the same speed (3.75 μm/s). The average indentation force was ~1 nN. Curves were obtained from at least nine cells under the same condition. The experiments for each condition typically lasted 30 min and never longer than 1 h. The work of detachment was derived from integrating the adhesive force over the distance traveled by the cantilever up to the point of the last bond rupture or complete cellular detachment. The detachment time was derived from detachment displacement times the retraction speed of the cantilever.

For the AFM analysis, we collected 15–20 force curves per each cell (thus, we obtained >100 measurements for each condition). For analysis, however, we used nine as the n value because the variation between cells was higher than the force curves collected for each cell. Therefore, instead of using a single cell and high number of force curves, say 100, we increased the number of cells to nine to have a better distribution and a better representative of the adhesion events.

Immunofluorescence microscopy

To visualize the long tethers, K562 CD11b/CD18 cells were transduced to express a membrane-bound marker conjugated to a green fluorescent protein (GFP) using the BacMam 2.0 CellLight Plasma Membrane-GFP system (Life Technologies). K562 CD11bCD18 cells were suspended in serum-free IMDM containing LA1 (15 μM) and were placed in glass bottom dishes (Wilco Wells; Amsterdam, Netherland) coated with ICAM-1. After 5 min, a bare AFM cantilever was used to displace the cell laterally. Confocal images of live cells were recorded with a scanning laser confocal microscope (Nikon A1R) system using a 60X oil immersion objective (N.A. 1.4) at 25°C. Z-stacks were generated from 0.2–0.5-μm thick serial sections. Maximum projection reconstructions from z-stacks were performed using Nikon's NIS-Elements image acquisition software. Imaging of the cells showed long membrane tethers when a mechanical force was applied to displace the cells activated with LA1. The images presented are representative of at least 20 cells analyzed for each condition from at least three independent experiments.

Statistical analysis

Data were analyzed using GraphPad Prism and compared with the Student's t-test or by one-way ANOVA with posthoc analysis, where appropriate. $P < 0.05$ was considered statistically significant.

RESULTS

Leukadherins increase CD11b/CD18-dependent cell adhesion to ICAM-1 and reduce deadhesion

We recently described integrin activation to be a useful mechanism for the development of novel antiinflammatory agents that reduce recruitment of inflammatory immune cells into tissues by increasing integrin CD11b/CD18-dependent cell adhesion to immobilized ligands (20,28). We identified a group of small molecule agonists targeting integrin CD11b/CD18, which we termed leukadherins (20,28,34). Among them, LA1 (Fig. 1 *A*) showed high affinity for CD11b/CD18 and increased cell adhesion to various ligands by binding to an allosteric pocket of the ligand-binding αA-domain (also known as αI-domain) of CD11b (CD11bA-domain, Fig. 1 *B*) (20). Increased cellular adhesion due to LA1-binding to CD11b/CD18 also resulted in significantly decreased cell migration. However, the mechanics of how LA1-mediated allosteric activation of CD11bA-domain modulates cellular adhesion and migration are not known. Here, we used SCFS to quantitatively investigate the biomechanical effects of LA1-mediated CD11b/CD18 activation on live cells.

First, we examined the relative increase in cell adhesion to immobilized physiologic ligand ICAM-1 that is mediated by known integrin agonist Mn^{2+} ions (35,36) and our novel allosteric agonist LA1 using K562 cells stably expressing WT CD11b/CD18 (K562 CD11b/CD18), which have full capacity and the machinery to link integrins to the

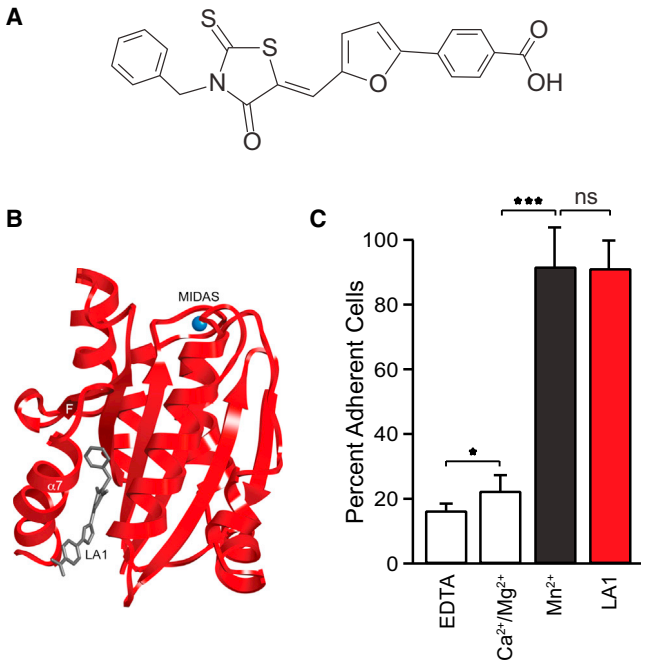

FIGURE 1 LA1 increases adhesion of integrin CD11b/CD18 to ICAM-1. (*A*) Chemical structure of LA1. (*B*) A cartoon showing a computationally generated model for LA1 (*gray stick model*) bound αA-domain (*red ribbon*) of the integrin CD11b/CD18. The metal ion (*blue sphere*) in the metal ion-dependent adhesion site (MIDAS) and the strands lining the activation sensitive allosteric site in αA are also labeled (*F*, α7). (*C*) A histogram showing relative adhesion of K562 CD11b/CD18 cells to immobilized ICAM-1 (as a percent of input cell number) in the presence of EDTA (10 mM), physiologic Ca^{2+} and Mg^{2+} ions (1 mM each, control), the nonselective integrin agonist Mn^{2+} (1 mM) or the agonist LA1 (15 μM). Data shown are mean ± SE (n = 3–6 replicates per condition) and are from one of at least three independent experiments. *$p < 0.05$, ***p < 0.0001, ns = not significant.

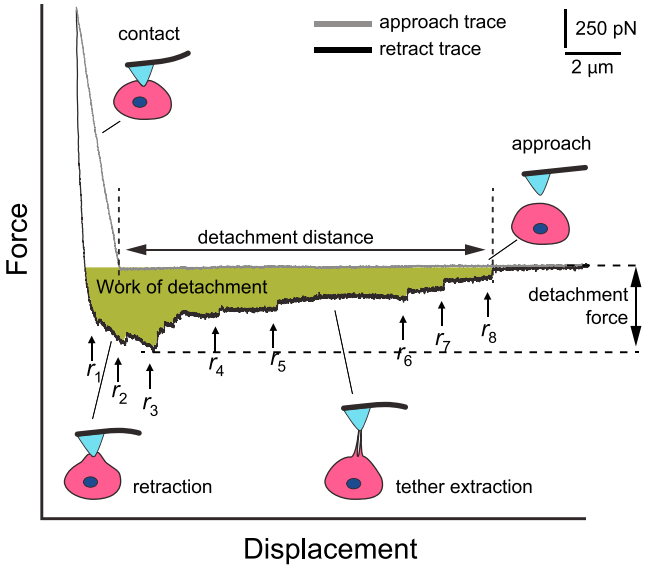

FIGURE 2 SCFS setup. Cartoon depiction of the experimental setup. A cell was immobilized on a tissue culture dish and the CD11b/CD18 ligand ICAM-1 was used to functionalize the AFM cantilever. The cartoon schematic also shows the principal events during an AFM force measurement: i), approach of the ICAM-1 functionalized AFM cantilever to an immobilized cell, ii), contact between the AFM cantilever tip and the cell, iii), retraction of the cantilever tip, from the cell surface, and iv), tether extraction during retraction of the cantilever tip. The gray trace was recorded during cantilever approach, whereas the black trace was recorded during retraction of the cantilever. To see this figure in color, go online.

cytoskeleton (29,37). Additionally, as has been shown previously, because the transfected integrin CD11b/CD18 is the only β2 integrin expressed on the surface of K562 CD11b/CD18 cells and since the K562 CD11b/CD18 cells constitutively express the WT CD11b/CD18 in a low affinity state (as in normal leukocytes) (29,37), these cells provide an ideal live cell system to examine the effects of CD11b/CD18 activation by various agonists (20,37). The ligand ICAM-1 was immobilized on the surface of multiwell microtiter plates and K562 CD11b/CD18 cells were added to the wells of the plates along with various agonists. The cells showed minimal basal adhesion to immobilized ICAM-1 in the presence of physiologic divalent cations (Ca^{2+} plus Mg^{2+}, each at 1 mM) over the control cells incubated in the absence of divalent ions (EDTA) (Fig. 1 *C*). Expectedly, the agonists Mn^{2+} and LA1 significantly increased adhesion of K562 CD11b/CD18 cells to ICAM-1.

Next, we used the K562 CD11b/CD18 cells in an AFM setup to directly measure the adhesive interaction between CD11b/CD18, upon activation with the two types of agonists, and the immobilized ICAM-1. Fig. 2 illustrates the AFM setup and the steps in the acquisition of the AFM force measurements. ICAM-1 was coupled to the end of an AFM cantilever and the K562 CD11b/CD18 cells were placed in a tissue culture dish. In this experiment, during the approach trace, the ICAM-1 functionalized AFM cantilever was lowered using a piezoelectric translator onto the surface of the cells. Following the tip-cell contact, continued expansion of the piezoelectric element pressed the flexible cantilever against the cells that resulted in an upward deflection of cantilever, which was continuously monitored to record mechanical force acting on the system at a given moment. Upon retraction of the piezoelectric translator, bonds formed between CD11b/CD18 and ICAM-1 resulted in a downward deflection of the cantilever. Cell adhesion was characterized using three parameters derived from AFM measurements: 1), the work of detachment 2), the detachment force and 3), detachment distance. The work of detachment is work done by the cantilever to detach the tip from the cell and was determined by integrating force over the distance curve. The detachment force is the maximum force generated by the cantilever to induce cell separation and the detachment distance is the distance over which the cantilever remained in contact with the cell. As shown in a series of traces in Fig. 3 *A*, activation of CD11b/CD18 with the nonspecific agonist Mn^{2+} and with the CD11b/CD18-agonist LA1 increased adhesion of

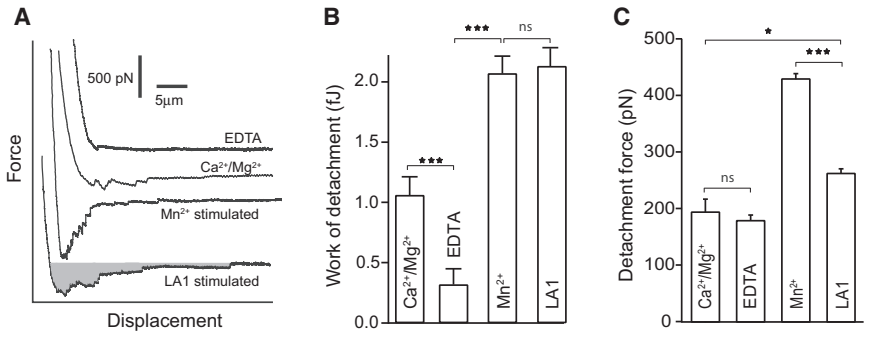

FIGURE 3 LA1 increases the work of deadhesion. (*A*) A series of representative AFM force curves carried out under identical conditions with K562 CD11b/CD18 cells interacting with ICAM-1 coated onto an AFM tip. The traces are from measurements carried out in buffers containing EDTA (10 mM), Ca^{2+} and Mg^{2+} ions (1 mM each), Mn^{2+} ions (1 mM), or LA1 (15 μM). (*B*) Histogram showing the work of detachment of K562 cells expressing CD11b/CD18 (K562 CD11b/CD18) from ICAM-1 in the presence of EDTA (10 mM), Ca^{2+} and Mg^{2+} ions (1 mM each), the agonist Mn^{2+} ions (1 mM), or the agonist LA1 (15 μM). Data shown are mean $\pm$ SE ($n = 9$ cells per condition). ***$p < 0.0001$, ns = not significant. (*C*) Histogram showing quantitation of the detachment force required to detach K562 CD11b/CD18 cells from ICAM-1 functionalized AFM cantilever in the presence of the control Ca^{2+} and Mg^{2+} ions (1 mM each), agonist Mn^{2+} ions (0.1 mM), or the agonist LA1 (15 μM). Data shown are mean $\pm$ SE ($n = 9$ cells per condition). *$p < 0.05$, ***$p < 0.0001$, ns = not significant.

K562 CD11b/CD18 cells to ICAM-1, as compared to cells incubated with divalent metal ion chelator EDTA that suppresses integrin ligand binding. This is evidenced by the larger maximum force required to detach the tip in the agonist-treated cells.

Fig. 3, *B* and *C*, show that the work of detachment and detachment force of K562 CD11b/CD18 cells to ICAM-1 under basal, physiologic concentration of Ca^{2+} and Mg^{2+} cations were both significantly higher than the corresponding values from cells treated with EDTA, where no integrin-mediated adhesion was detected in the conventional adhesion assay (Fig. 1 *C*). As predicted by the conventional adhesion assay, both small molecule agonist LA1 and nonphysiological adhesion promoter, Mn^{2+}, significantly enhanced the work of detachment and detachment force of CD11b/CD18 expressing K562 cells to ICAM-1, as compared to the cells adhering under the basal condition (1 mM each of Ca^{2+} and Mg^{2+} cations). To test the specificity of the interaction between ICAM-1 and CD11b/CD18 in our assay system, we also conducted similar measurements on the nontransfected, parental K562 cell line (Fig. S1 in the Supporting Material). In all test conditions performed on the K562 cells (EDTA, Ca^{2+} and Mg^{2+}, Mn^{2+}, and LA1), the detachment force and work of detachment were significantly less than the observed values with activated K562 CD11b/CD18 cells and were similar to the levels obtained with K562 CD11b/CD18 cells treated with EDTA (basal level). These control measurements ensured that most of the unbinding events seen in the force curves of the CD11b/CD18 expressing K562 cells were due to the specific adhesive interaction between CD11b/CD18 and ICAM-1. Thus, the results presented here suggest that LA1 significantly increases the energy required for detachment.

To determine if the area of tip-cell contact is the same for the different experimental condition, Young's modulus of cells were measured (Fig. S2). Because cells treated with Mn^{2+} were stiffer than cells under basal condition or treated with LA1, the area of tip-cell contact at constant indentation is less for the Mn^{2+}-treated cells. The addition of agonist LA1 did not significantly change Young's modulus of K562 CD11b/CD18 cells, as compared to cells in basal, control conditions (Ca^{+2}/Mg^{+2}). However, the addition of agonist Mn^{2+} made the cells stiffer, an observation that is consistent with published results (38). For a given indentation force, an increase in Young's modulus reduces the contact area and the number of the bonds formed. Our force measurements revealed that there was a significant increase in cell adhesion in the presence of Mn^{2+} even though the contact area was reduced.

LA1 increases cell adhesion via long membrane tethers

A closer examination of the AFM cell adhesion measurements revealed that the ICAM-1 functionalized AFM cantilever detached from the K562 CD11b/CD18 cell surface via a series of ruptures as seen by the sharp vertical transitions in the retraction curve (Fig. 3 *A*). Each rupture, denoted by an arrow in Fig. 2, corresponds to the breakage of at least one single bond between the integrin CD11b/CD18 and ICAM-1. As reported previously, the AFM measurements also revealed two distinct types of connections in integrin-mediated cell adhesion: 1), cytoskeletal (CSK)-anchored and 2), membrane-tethered bonds (39). The CSK-anchored integrins are bound to the cellular cytoskeleton such that the anchor bond strength is greater than the strength of the adhesive bond between CD11b/CD18 and ICAM-1. Consequently, as the ICAM-1 functionalized AFM cantilever is withdrawn from the cell surface, the adhesive bond between CD11b/CD18 and ICAM-1 unbinds before the CSK-anchors rupture. Thus, the unbinding of CSK-anchored CD11b/CD18-ICAM-1 complexes, which typically occurred during early cell detachment, is coupled to the extension of the elastic cytoskeletal elements and is preceded by an increase in the pulling force (e.g., r1, r2, and r3 in Fig. 2). By contrast, the membrane-tethered integrins are not anchored to the cytoskeleton or are only weakly

associated with it, such that this weak cytoskeletal association breaks before the adhesive interaction between CD11b/CD18 and ICAM-1. In such a case, membrane tethers were formed when the integrins were pulled from the cell, see Fig. 5 *C*. Due to the viscous properties of the membrane tethers, membrane-tethered CD11b/CD18:ICAM-1 ruptures exhibit a long constant force plateau before its dissociation (e.g., r4, r5, and r6 in Fig. 2). Fig. 4 reveals that stimulation of K562 CD11b/CD18 cells with Mn^{2+} increased the occurrence of CSK-anchored ruptures and membrane-tethered ruptures by the factors of 1.5 and 4, respectively, over cells incubated with physiologic 1 mM Ca^{2+} and Mg^{2+} ion containing buffer. This result was expected because Mn^{2+} ions activate all of the integrins on the cell surface regardless of their anchorage type. Activation of CD11b/CD18 on K562 cells with LA1, similar to its stimulation with Mn^{2+} ions, also showed increased activation of the membrane-tethered integrins, which resulted in a fourfold increase in the number of tether bond ruptures, as compared to the tether bond ruptures in the control Ca^{2+} and Mg^{2+} cells. However, surprisingly, the agonist LA1 did not affect the occurrence of CSK-anchored ruptures in these measurements, as was observed with the Mn^{2+}-treated cells. A comparison between the fraction of CSK-bonds and membrane tether bonds between the Mn^{2+} and LA1 conditions clearly shows that LA1 increases cell adhesion via a mechanism distinct from Mn^{2+} and that it primarily mediates its adhesive effects by increasing the number of membrane tether bonds (Fig. 4 *B*).

During the retraction of the ICAM-1 functionalized cantilever from LA1-treated K562 CD11b/CD18 cells, we also observed that the cell is highly stretched, with elongations of several microns, possibly stemming from tether formations (40). Quantitation of the distance required to detach ICAM-1 functionalized AFM cantilevers from the K562 CD11b/CD18 cells under various conditions showed that the detachment distance increased significantly when the cells are activated with LA-1, as compared to the nonactivated control cells. However, it remained unchanged for cells activated with Mn^{2+} ions over nonactivated cells (Fig. 5 *A*). The detachment time also increased in LA1-activated cells, but not Mn^{2+} activated cells, as compared to the nonactivated cells. To visualize the long tethers, K562 CD11b/CD18 cells were transfected with a membrane-bound marker conjugated to a GFP (the BacMam 2.0 CellLight Plasma Membrane-GFP marker) and the cells were placed on ICAM-1-coated surfaces. Confocal imaging of the cells showed long membrane tethers when a mechanical force was applied to displace the cells activated with LA1 (Fig. 5 *C*) versus the cells at rest (Fig. 5 *B*). Taken together, these results suggest that the mechanism of LA1-mediated increased in cell adhesion might be distinct from that of the nonspecific integrin agonist Mn^{2+} ions and that the agonist LA1 primarily mediates its adhesive effects by increasing the number of membrane tether bonds versus primarily the CSK-bond mediated increase in adhesion imparted by the Mn^{2+} ions.

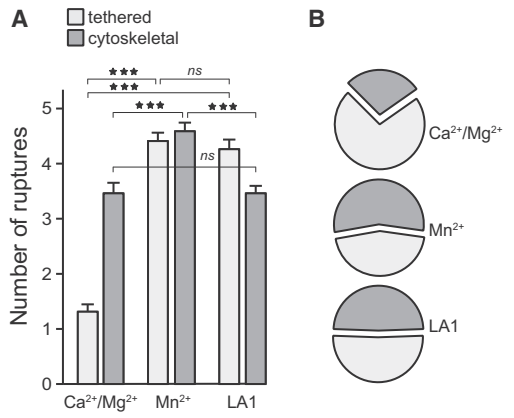

FIGURE 4 LA1 mediates adhesion of CD11b/CD18 cells via membrane tether bonds. (*A*) A histogram showing quantitation of the number and the type of ruptures (CSK-bonds and membrane tether bonds) during the detachment of CD11b/CD18 expressing K562 cells from ICAM-1 functionalized AFM cantilever in the presence of physiologic Ca^{2+} and Mg^{2+} ions (1 mM each), Mn^{2+} ions (1 mM), or LA1 (15 μM). Data shown are mean ± SE ($n = 9$ cells per condition). ***$p < 0.0001$, ns = not significant. (*B*) Pie charts from the data presented in 4*A* showing the relative percentage of CSK bond ruptures versus membrane tether bond ruptures during the detachment of K562 CD11b/CD18 cells from ICAM-1 in cells stimulated with agonists Mn^{2+} ions or LA1.

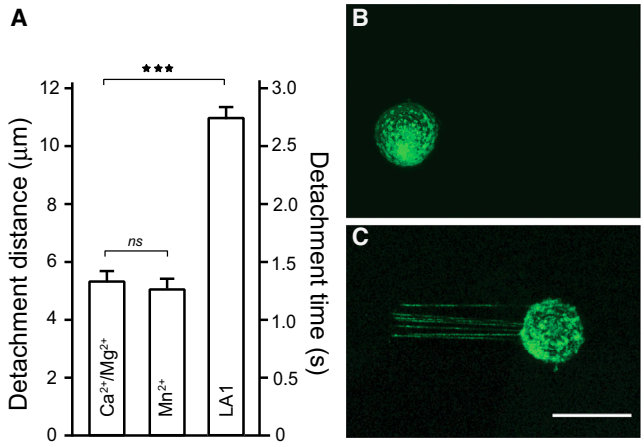

FIGURE 5 The agonist LA1 increases membrane tethers. (*A*) A histogram showing quantitation of the distance required to detach CD11b/CD18 expressing K562 cells from ICAM-1 functionalized AFM cantilever and the detachment time in the presence of control physiologic Ca^{2+} and Mg^{2+} ions (1 mM each), agonist Mn^{2+} ions (1 mM), or the agonist LA1 (15 μM). Data shown are mean ± SE ($n = 9$ cells per condition). ***$p < 0.0001$, ns = not significant. (*B* and *C*) Confocal microscopy images of membrane tethers on LA1-activated K562 CD11b/CD18 cells. K562 CD11b/CD18 cells transfected with a membrane-bound GFP marker (CellLight Plasma Membrane-GFP, *green*) were placed on ICAM-1 coated surfaces and were either not disturbed (*B*) or a mechanical force was applied to displace the cells activated with LA1 (15 μM) in the direction from left to right (*C*). A representative fluorescent image (*C*) revealed presence of increasing number of long membrane tethers on the affected cells. Scale bar represents 20 μm.

LA1 increases CD11b/CD18-dependent neutrophil adhesion via tether bonds

CD11b/CD18 is highly expressed on neutrophils and mediates the various biological functions of these cells. To examine the biophysical mechanism of how LA1 mediates its effects on the adhesion and migration of primary neutrophils, we used murine neutrophils in our cell force spectroscopy setup. Because, under basal conditions, neutrophils express significant levels of $\beta 2$ integrin CD11a/CD18 (LFA-1, $\alpha L\beta 2$) and CD11b/CD18 (27), and since ICAM-1 is also a ligand for CD11a/CD18, we decided to use neutrophils from LFA-1 knock out animals (LFA-$1^{-/-}$) in these studies so as to solely focus on the specific CD11b/CD18: ICAM-1 interaction. As expected, in adhesion assays, the LFA-$1^{-/-}$ neutrophils showed significantly enhanced adhesion to immobilized ICAM-1 upon stimulation with agonists Mn^{2+} ions or LA1, as compared to the cell adhesion under basal, physiologic buffer conditions (Ca^{2+} and Mg^{2+} ions) or in the presence of EDTA (Fig. 6 *A*). WT B6 neutrophils showed similar results (Fig. S3 *A*).

Increasing CD11b/CD18-mediated cell adhesion with LA1 decreases neutrophil migration and chemotaxis (20). Both murine WT B6 neutrophils (Fig. S3, *B* and *C*), and the LFA-$1^{-/-}$ neutrophils (Fig. 6, *B* and *C*), showed significantly reduced lateral migration in response to a gradient of chemokine peptide fMLP in the presence of agonists Mn^{2+} ions or LA1 as compared to their migration under basal, physiologic buffer conditions (Ca^{2+} and Mg^{2+} ions). Neutrophils, in response to chemokine signaling, polarize and form distinct front edge (lamellipodia) and a trailing/rear edge (uropod) to start migration (7,41). A forward migration of the cell involves uropod elongation, via long membrane tethers, and subsequent retraction (42) and increasing integrin-mediated cell adhesion results in delayed uropod deadhesion and long membrane tethers (43). Previously, we determined that the neutrophils chemotaxing in the presence of LA1 also show elongated tethers at the uropods (20), suggesting increased number and/or length of membrane tethers as a potential mechanism for how the agonist LA1 might be mediating its effects on neutrophil migration. To investigate this further, we used AFM to quantitatively measure the effects of agonists Mn^{2+} and LA1 on enhanced anchorage of neutrophil cell-surface expressed CD11b/CD18 to AFM tip immobilized ICAM-1. As with K562 CD11b/CD18 cells, the incubation of LFA-$1^{-/-}$ neutrophils with nonspecific integrin agonist Mn^{2+} or with the CD11b/CD18 agonist LA1 resulted in a similar increase in the detachment energy of LFA-$1^{-/-}$ neutrophils to ICAM-1 (~3.5-fold), as compared to the detachment energy observed under basal, physiologic buffer conditions (Ca^{2+} and Mg^{2+} cations) (Fig. 7 *A*). Like K562 CD11b/CD18 cells, the LA1-stimulated neutrophils were also highly stretched, with increased membrane elongations, likely due to increased tether formations. Quantitation of the distance required to detach the ICAM-1 coated AFM cantilever tips from the LFA-$1^{-/-}$ neutrophils and the detachment time also showed that the detachment distance (and time) increased significantly upon cell activation with LA-1, although little such increase is seen upon activation with Mn^{2+} ions (Fig. 7 *B*). Analysis of the force required for the tip detachment (*detachment force*, Fig. 7 *C*) showed that integrin activation with either Mn^{2+} or LA1 increased the detachment force required for the tip release, as compared to the nonactivated condition. However, although activation with Mn^{2+} resulted in a large increase in the force required, cells activated with LA1 required a substantially reduced level of detachment force, confirming a stronger interaction between the Mn^{2+} activated CD11b/CD18 and ICAM-1. A detailed analysis of the AFM profiles again revealed that, like with K562 CD11b/CD18 cells, the agonist Mn^{2+} significantly increased the CSK-anchored ruptures over the cells incubated with physiologic 1 mM Ca^{2+} and Mg^{2+} ion

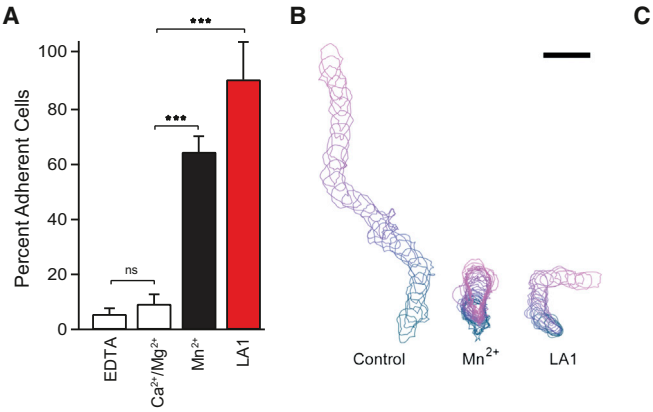

FIGURE 6 LA1 increases LFA-$1^{-/-}$ neutrophil adhesion and decreases cell migration. (*A*) A histogram showing adhesion of LFA-$1^{-/-}$ neutrophils to immobilized ICAM-1 (normalized to input cell number) in the presence of EDTA (10 mM), physiologic Ca^{2+} and Mg^{2+} ions (1 mM each), the nonselective integrin agonist Mn^{2+} (0.1 mM), or the agonist LA1 (15 μM). Data shown are mean ± SE ($n = 3$ replicates per condition) and are from one of at least three independent experiments. ***$p < 0.0001$, ns = not significant. (*B*) Representative overlay plots showing analysis of migrating LFA-$1^{-/-}$ neutrophils in Zigmond chambers in response to an fMLP gradient and in media containing physiologic Ca^{2+} and Mg^{2+} ions (1 mM each), the nonselective integrin agonist Mn^{2+} (0.1 mM), or the agonist LA1 (15 μM). The overlay plots were created from the outlines of migrating cells at various time points from time-lapse video microscopy. The directionality of the cell movement is from bottom to the top. Scale bar represents 14 μm. (*C*) A bar graph showing the mean displacement of LFA-$1^{-/-}$ neutrophils during migration after quantitative analyses of the data shown in 6*B*. Data shown are mean ± SE ($n = 75$–100 cells per condition). ***$p < 0.0001$, ns = not significant.

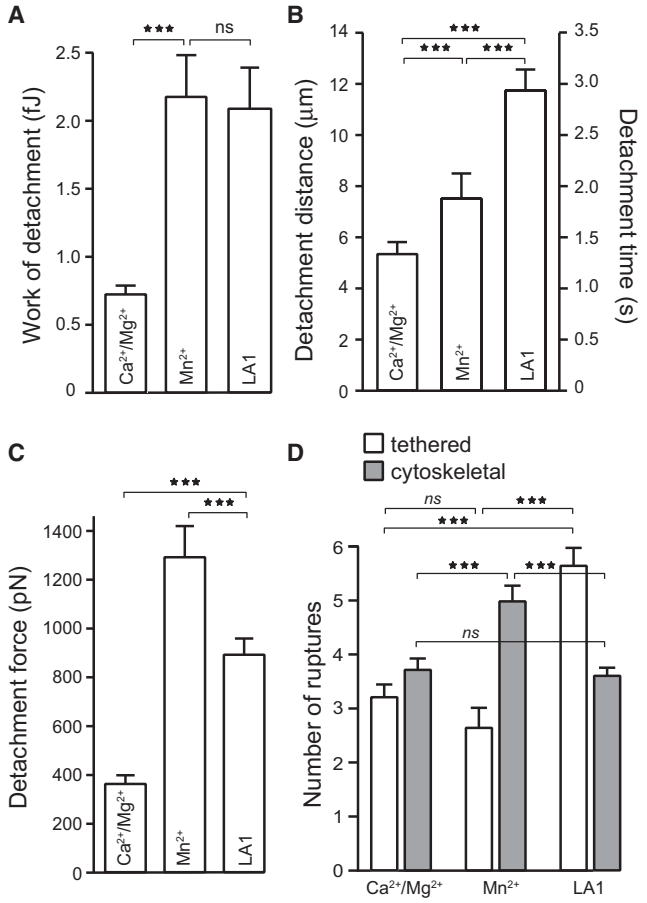

FIGURE 7 LA1 increases the detachment energy and the rupture distance of neutrophils bound to ICAM-1. (*A*) A histogram showing the work of detachment of LFA-$1^{-/-}$ neutrophils from ICAM-1 in the presence of physiologic Ca^{2+} and Mg^{2+} ions (1 mM each), the nonspecific agonist Mn^{2+} ions (0.1 mM), or the agonist LA1 (15 μM). Data shown are mean ± SE ($n = 6$–9 cells per condition). ***$p < 0.0001$, ns = not significant. (*B*) A histogram showing quantitation of the distance required to detach LFA-$1^{-/-}$ neutrophils from ICAM-1 functionalized AFM cantilever and the detachment time in the presence of the control Ca^{2+} and Mg^{2+} ions (1 mM each), agonist Mn^{2+} ions (0.1 mM), or the agonist LA1 (15 μM). Data shown are mean ± SE ($n = 6$ to 9 cells per condition). ***$p <$ 0.0001. (*C*) A histogram showing quantitation of the detachment force required to detach LFA-$1^{-/-}$ neutrophils from ICAM-1 functionalized AFM cantilever in the presence of the control Ca^{2+} and Mg^{2+} ions (1 mM each), agonist Mn^{2+} ions (0.1 mM), or the agonist LA1 (15 μM). Data shown are mean ± SE ($n = 6$ to 9 cells per condition). ***$p <$ 0.0001. (*D*) A histogram showing quantitation of the number and the type of ruptures (CSK-bonds and membrane tether bonds) during the detachment of LFA-$1^{-/-}$ neutrophils from ICAM-1 in the presence of Ca^{2+} and Mg^{2+} ions (1 mM each), Mn^{2+} ions (0.1 mM), or LA1 (15 μM). Data shown are mean ± SE ($n = 6$–9 cells per condition). ***$p < 0.0001$, ns = not significant.

containing buffer, whereas LA1 primarily increased the occurrence of membrane tethers (Fig. 7 *D*). In all, the data clearly suggest that the two types of agonists differentially mediate CD11b/CD18 dependent adhesion to ICAM-1 and that LA1 primarily mediates its effects by increasing the number of membrane tethers.

DISCUSSION

LA1 is a member of a family of recently described small molecules (termed leukadherins) that bind to the ligand binding αA-domain of integrin CD11b/CD18, allosterically stimulating CD11b/CD18-dependent cell adhesion and reducing cell migration (20). LA1 administration in vivo also results in increased neutrophil adhesion, significantly decreased neutrophil migration, and tissue recruitment and reduced inflammatory injury. This suggested that CD11b/CD18 agonists are potential therapeutics for treating a variety of inflammatory conditions in humans. However, whether all integrin agonists, including known nonspecific agonists, such as Mn^{2+} ions, could be potential therapeutics or whether small molecule allosteric agonists, such as LA1, use a different mechanism to modulate cell adhesion, is not known and is important to investigate before such reagents can be moved forward in the drug development pipeline. Here, we used AFM-based single-cell spectroscopy measurements to quantitatively establish the biophysical mechanism of how LA1 affects cell adhesion and migration. Using an immortalized cell line (K562 cells) we found that both, the known integrin agonist Mn^{2+} and the novel, to our knowledge, small molecule agonist LA1, significantly enhanced the binding and the detachment energy of CD11b/CD18 to ICAM-1 over control, basal conditions. The AFM measurements revealed that there are two populations of CD11b/CD18 expressed on the surface of cells: one population is anchored to the cytoskeleton (via CSK-anchored bonds, where the strength of the integrin-cytoskeletal linkage bond is greater than the strength of the linkage between CD11b/CD18 and ligand (e.g., ICAM-1)) and a second population that is weakly associated with the plasma membrane such that its cytoskeletal linkage unravels before the adhesive bond between CD11b/CD18 and its ligand, thus forming membrane tethers when pulled. These two populations of CD11b/CD18 employ different biophysical mechanisms for cell adhesion and migration. A closer examination of the AFM-traces showed that LA1 primarily increased the occurrence of membrane tether bonds, whereas Mn^{2+} additionally increased CSK-anchored bonds, suggesting that the two types of agonists may differentially mediate the increase in cellular adhesivity via integrins. Given that CD11b/CD18 is highly expressed in neutrophils and mediates a majority of its biological functions, we also investigated the mechanism of how the two types of agonists stimulate CD11b/CD18-mediated cell adhesion to ICAM-1 in these primary cells. Additionally, as the neutrophils also express integrin LFA1, another cellular receptor for ICAM-1 and an integrin that is highly homologous to CD11b/CD18, we used neutrophils from LFA1 knockout animals (LFA$1^{-/-}$), in addition to the WT neutrophils, to focus solely on the CD11b/CD18:ICAM-1 interaction. In static adhesion assays, both Mn^{2+} and LA1 significantly increased the adhesion of neutrophils to immobilized

ICAM-1 and the AFM measurements confirmed that both also equally increased the detachment energy of CD11b/CD18 to ICAM-1 over nonactivated cells. However, as with K562 CD11b/CD18 cells, LA1 activated cells showed much longer detachment distances and took a longer time to detach the ICAM-1-coated AFM tips, but showed significantly reduced detachment force, as compared to the Mn^{2+} stimulated cells. Comparison of the type of cellular attachment confirmed that, like with K562 CD11b/CD18 cells, LA1 primarily increased the number of membrane-tether bonds to increase CD11b/CD18:ICAM-1 binding, whereas Mn^{2+} additionally induced the CSK-anchored bonds.

Differences between LA1 and Mn^{2+} activation mechanisms can be rationalized in a model where the majority of the inactive integrin CD11b/CD18 molecules of the resting cells are mobile and do not strongly associate with the cytoskeleton. For example, it was recently shown that 95% of LFA1 in THP-1 cells is primarily organized in nanoclusters and is highly mobile (44). Therefore, our proposed model for the mechanism of CD11b activation via the two types of agonists as follows (*schematically depicted* in Fig. 8). LA1 specifically activates resting integrins, which are highly mobile and are primarily not associated with the cellular cytoskeleton, to bind to ligand ICAM-1, thereby enhancing the lifetime but not the force of the adhesive bond and causing tethers to form. The nonspecific agonist Mn^{2+}, by altering the extracellular CD11b/CD18 conformation to a fully active, highly adhesive state, additionally enhanced integrin-cytoskeletal linkage. We recently noted, using conformation-sensitive antibodies, that LA1-mediated CD11b/CD18 activation results in local, rather than global, conformational changes in the integrin dimer (21), whereas activation with Mn^{2+} provided global conformational changes, consistent with the observations here. Bakker et al. also noted a reduction in LFA-1 motility upon cell activation. This would explain the increase in the number of CSK ruptures in the AFM force measurements. Additionally, it has been reported that integrins in high affinity conformation bind their ligands primarily via cytoskeletal linkages, whereas such a CSK-linkage is not needed for integrin priming and adhesion mediated via intermediate affinity conformation of integrins (45,46). This would suggest that LA1-mediated CD11b/CD18 activation leads to integrin priming and conversion to an intermediate affinity conformation, also consistent with our recent findings using conformation-specific antibodies (21). The results indicate that these two types of agonists differentially transduce mechanical signals to inside the cells.

In addition to an increase in the number of tethers formed upon LA1 treatment of K562 CD11b/CD18 cells and the neutrophils, we also noted that there is an increase in the detachment distance, which we attribute to an increase in the length and lifetime of the last membrane tether to rupture. The lifetime of this last tether increased from 1.5 s to 3.5 s after LA1 treatment. The lifetime of these tethers are significantly longer than expected for a membrane tether supported by a single CD11b/CD18:ICAM-1 complex at the pulling force of 25 pN. We estimate (*based on derivation* in Fig. S4 (47,48);) that there are between 7 and 20 CD11b/CD18:ICAM-1 complexes supporting the last tether of resting and LA1 treated cells, respectively. Interestingly, the detachment distance of Mn^{2+}-activated cells (~6 um) was significantly shorter than measurements from LA1-treated cells (~12 um). We attribute this difference to the strong coupling of CD11b/CD18 to the cytoskeleton, which reduces the number of CD11b/CD18 available for elongation of membrane tethers. Consequently, Mn^{2+}-activated neutrophils formed strong CSK bonds with large detachment forces (Fig. 7) that were difficult for a migrating cell to rupture; hence they were less mobile (Fig. 6 *C*). LA1-treated cells formed long tethers, but their detachment force

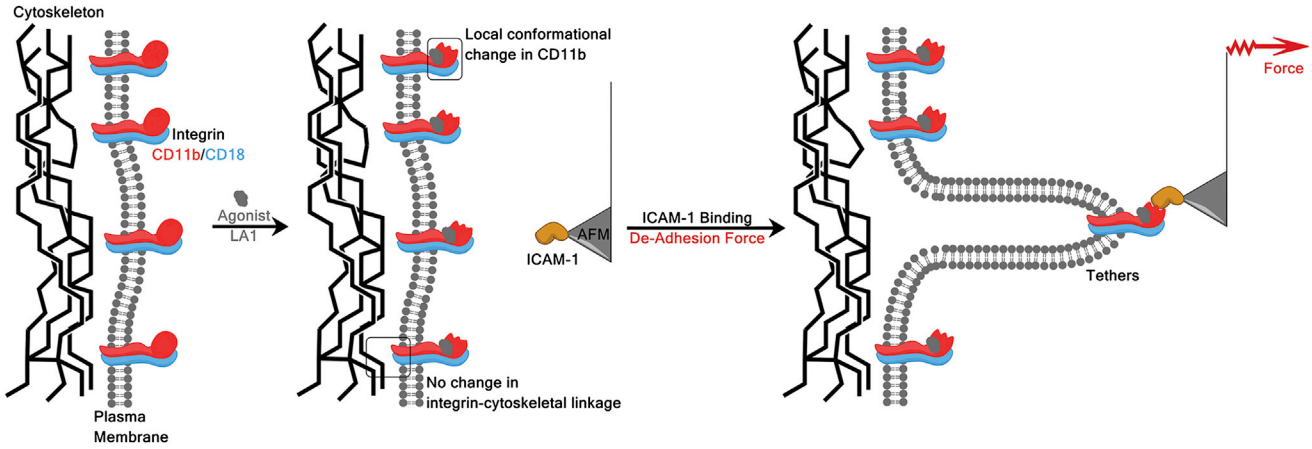

FIGURE 8 LA1 mediates its effects on CD11b/CD18-dependent cell adhesion by increasing the membrane tether bonds. A cartoon model depicting the effect of LA1 binding and CD11b/CD18 activation showing that LA1 binding to the ligand binding αA-domain of CD11b/CD18 primarily enhances the adhesion of CD11b/CD18-expressing cells to ICAM-1 via membrane tether bonds and not the cytoskeletal linkages.

was weaker than that of Mn^{2+}-treated cells. Hence, it was easier for LA1-treated cells to overcome this traction and cells were more motile (Fig. 6 *C*).

In summary, we show here that different agonists of CD11b/CD18 use different mechanisms to couple integrin activation to the cellular machinery. Agonist LA1 primarily increased the number of integrin membrane-tether bonds, whereas agonist Mn^{2+} additionally induced the integrin-cytoskeletal linkages. In vivo, the formation of these long membrane tethers may provide the structural units for the arrest of rolling leukocytes within the blood vessels.

SUPPORTING MATERIAL

Four figures are available at http://www.biophysj.org/biophysj/supplemental/S0006-3495(13)01185-5.

We thank Dony Maiguel, Alexander Braley, and Tristan Hays for generous help and discussions with the cell-based assays.

This work was supported in part by National Institutes of Health (NIH) Grants R01-DK084195 (to V.G.), R01-HL109582 (to V.G.), and R01-GM086808 (to V.T.M.), American Heart Association Grant 11GRN7660018 (to V.G.) and a National Science Foundation (NSF) Grant MRI 0722372, a James & Esther King Biomedical Research Program Grant 24157, and a Woman Cancer Association Grant (to V.T.M.).

V.G. is an inventor of pending patents related to the study, and V.G. and the University of Miami have the potential for financial benefit from their future commercialization. The pending patents have been licensed to Adhaere Pharmaceuticals, Inc., a company cofounded by V.G. The authors have no additional financial interests.

REFERENCES

1. Simon, D. I., Z. Dhen, …, C. Rogers. 2000. Decreased neointimal formation in Mac-1(-/-) mice reveals a role for inflammation in vascular repair after angioplasty. *J. Clin. Invest.* 105:293–300.
2. Arnaout, M. A., R. F. Todd, 3rd, …, H. R. Colten. 1983. Inhibition of phagocytosis of complement C3- or immunoglobulin G-coated particles and of C3bi binding by monoclonal antibodies to a monocyte-granulocyte membrane glycoprotein (Mol). *J. Clin. Invest.* 72:171–179.
3. Li, R., and M. A. Arnaout. 1999. Functional analysis of the beta 2 integrins. *Methods Mol. Biol.* 129:105–124.
4. Dustin, M. L., R. Rothlein, …, T. A. Springer. 1986. Induction by IL 1 and interferon-gamma: tissue distribution, biochemistry, and function of a natural adherence molecule (ICAM-1). *J. Immunol.* 137:245–254.
5. Ley, K., C. Laudanna, …, S. Nourshargh. 2007. Getting to the site of inflammation: the leukocyte adhesion cascade updated. *Nat. Rev. Immunol.* 7:678–689.
6. Schmidtke, D. W., and S. L. Diamond. 2000. Direct observation of membrane tethers formed during neutrophil attachment to platelets or P-selectin under physiological flow. *J. Cell Biol.* 149:719–730.
7. Sundd, P., E. Gutierrez, …, K. Ley. 2010. Quantitative dynamic footprinting microscopy reveals mechanisms of neutrophil rolling. *Nat. Methods.* 7:821–824.
8. Rieu, P., T. Sugimori, …, M. A. Arnaout. 1996. Solvent-accessible residues on the metal ion-dependent adhesion site face of integrin CR3 mediate its binding to the neutrophil inhibitory factor. *J. Biol. Chem.* 271:15858–15861.
9. Diamond, M. S., D. E. Staunton, …, T. A. Springer. 1991. Binding of the integrin Mac-1 (CD11b/CD18) to the third immunoglobulin-like domain of ICAM-1 (CD54) and its regulation by glycosylation. *Cell.* 65:961–971.
10. Diamond, M. S., D. E. Staunton, …, T. A. Springer. 1990. ICAM-1 (CD54): a counter-receptor for Mac-1 (CD11b/CD18). *J. Cell Biol.* 111:3129–3139.
11. Yonekawa, K., and J. M. Harlan. 2005. Targeting leukocyte integrins in human diseases. *J. Leukoc. Biol.* 77:129–140.
12. Jaeschke, H., A. Farhood, …, C. W. Smith. 1993. Functional inactivation of neutrophils with a Mac-1 (CD11b/CD18) monoclonal antibody protects against ischemia-reperfusion injury in rat liver. *Hepatology.* 17:915–923.
13. Rogers, C., E. R. Edelman, and D. I. Simon. 1998. A mAb to the beta2-leukocyte integrin Mac-1 (CD11b/CD18) reduces intimal thickening after angioplasty or stent implantation in rabbits. *Proc. Natl. Acad. Sci. USA.* 95:10134–10139.
14. Wilson, I., A. M. Gillinov, …, D. E. Cameron. 1993. Inhibition of neutrophil adherence improves postischemic ventricular performance of the neonatal heart. *Circulation.* 88:II372–II379.
15. Argenbright, L. W., L. G. Letts, and R. Rothlein. 1991. Monoclonal antibodies to the leukocyte membrane CD18 glycoprotein complex and to intercellular adhesion molecule-1 inhibit leukocyte-endothelial adhesion in rabbits. *J. Leukoc. Biol.* 49:253–257.
16. Dove, A. 2000. CD18 trials disappoint again. *Nat. Biotechnol.* 18:817–818.
17. Harlan, J. M., and R. K. Winn. 2002. Leukocyte-endothelial interactions: clinical trials of anti-adhesion therapy. *Crit. Care Med.* 30 (*Suppl*):S214–S219.
18. Molloy, E. S., and L. H. Calabrese. 2009. Therapy: targeted but not trouble-free: efalizumab and PML. *Nat. Rev. Rheumatol.* 5:418–419.
19. Allison, M. 2010. PML problems loom for Rituxan. *Nat. Biotechnol.* 28:105–106.
20. Maiguel, D., M. H. Faridi, …, V. Gupta. 2011. Small molecule-mediated activation of the integrin CD11b/CD18 reduces inflammatory disease. *Sci. Signal.* 4:1–14.
21. Noth, I., J. J. Hutter, …, L. P. Carter. 1993. Spinal epidural hematoma in a hemophilic infant. *Am. J. Pediatr. Hematol. Oncol.* 15:131–134.
22. Peter, K., M. Schwarz, …, C. Bode. 2001. Intrinsic activating properties of GP IIb/IIIa blockers. *Thromb. Res.* 103 (*Suppl*):S21–S27.
23. Mahalingam, B., K. Ajroud, …, M. A. Arnaout. 2011. Stable coordination of the inhibitory Ca2+ ion at the metal ion-dependent adhesion site in integrin CD11b/CD18 by an antibody-derived ligand aspartate: implications for integrin regulation and structure-based drug design. *J. Immunol.* 187:6393–6401.
24. Vuorte, J., P. J. Lindsberg, …, H. Repo. 1999. Anti-ICAM-1 monoclonal antibody R6.5 (Enlimomab) promotes activation of neutrophils in whole blood. *J. Immunol.* 162:2353–2357.
25. Peter, K., M. Schwarz, and C. Bode. 2002. Activating effects of GPIIb/IIIa blockers: an intrinsic consequence of ligand-mimetic properties. *Circulation.* 105:E180–E181.
26. Hutter, J. L., and J. Bechhoefer. 1993. Calibration of atomic-force microscope tips. *Rev. Sci. Instrum.* 64:1868–1873.
27. Ding, Z. M., J. E. Babensee, …, C. M. Ballantyne. 1999. Relative contribution of LFA-1 and Mac-1 to neutrophil adhesion and migration. *J. Immunol.* 163:5029–5038.
28. Park, J. Y., M. A. Arnaout, and V. Gupta. 2007. A simple, no-wash cell adhesion-based high-throughput assay for the discovery of small-molecule regulators of the integrin CD11b/CD18. *J. Biomol. Screen.* 12:406–417.
29. Gupta, V., A. Gylling, …, M. A. Arnaout. 2007. The beta-tail domain (betaTD) regulates physiologic ligand binding to integrin CD11b/CD18. *Blood.* 109:3513–3520.
30. Faridi, M. H., D. Maiguel, …, V. Gupta. 2010. High-throughput screening based identification of small molecule antagonists of integrin CD11b/CD18 ligand binding. *Biochem. Biophys. Res. Commun.* 394:194–199.

31. Szczur, K., H. Xu, …, M. D. Filippi. 2006. Rho GTPase CDC42 regulates directionality and random movement via distinct MAPK pathways in neutrophils. *Blood.* 108:4205–4213.

32. Zigmond, S. H. 1988. Orientation chamber in chemotaxis. *Methods Enzymol.* 162:65–72.

33. Bell, G. I. 1978. Models for the specific adhesion of cells to cells. *Science.* 200:618–627.

34. Faridi, M. H., D. Maiguel, …, V. Gupta. 2009. Identification of novel agonists of the integrin CD11b/CD18. *Bioorg. Med. Chem. Lett.* 19:6902–6906.

35. Altieri, D. C. 1991. Occupancy of CD11b/CD18 (Mac-1) divalent ion binding site(s) induces leukocyte adhesion. *J. Immunol.* 147:1891–1898.

36. Dransfield, I., C. Cabañas, …, N. Hogg. 1992. Divalent cation regulation of the function of the leukocyte integrin LFA-1. *J. Cell Biol.* 116:219–226.

37. Ortlepp, S., P. E. Stephens, …, M. K. Robinson. 1995. Antibodies that activate beta 2 integrins can generate different ligand binding states. *Eur. J. Immunol.* 25:637–643.

38. Wojcikiewicz, E. P., X. Zhang, …, V. T. Moy. 2003. Contributions of molecular binding events and cellular compliance to the modulation of leukocyte adhesion. *J. Cell Sci.* 116:2531–2539.

39. Chu, C., E. Celik, …, V. T. Moy. 2013. Elongated membrane tethers, individually anchored by high affinity $\alpha 4\beta 1$/VCAM-1 complexes, are the quantal units of monocyte arrests. *PLoS ONE.* 8:e64187.

40. Benoit, M., and H. E. Gaub. 2002. Measuring cell adhesion forces with the atomic force microscope at the molecular level. *Cells Tissues Organs (Print).* 172:174–189.

41. Sengupta, K., H. Aranda-Espinoza, …, D. Hammer. 2006. Spreading of neutrophils: from activation to migration. *Biophys. J.* 91:4638–4648.

42. Hyun, Y. M., R. Sumagin, …, M. Kim. 2012. Uropod elongation is a common final step in leukocyte extravasation through inflamed vessels. *J. Exp. Med.* 209:1349–1362.

43. Park, E. J., J. R. Mora, …, M. Shimaoka. 2007. Aberrant activation of integrin alpha4beta7 suppresses lymphocyte migration to the gut. *J. Clin. Invest.* 117:2526–2538.

44. Bakker, G. J., C. Eich, …, M. F. Garcia-Parajo. 2012. Lateral mobility of individual integrin nanoclusters orchestrates the onset for leukocyte adhesion. *Proc. Natl. Acad. Sci. USA.* 109:4869–4874.

45. Shao, B., T. Yago, …, R. P. McEver. 2012. Signal-dependent slow leukocyte rolling does not require cytoskeletal anchorage of P-selectin glycoprotein ligand-1 (PSGL-1) or integrin $\alpha L\beta 2$. *J. Biol. Chem.* 287:19585–19598.

46. Schürpf, T., and T. A. Springer. 2011. Regulation of integrin affinity on cell surfaces. *EMBO J.* 30:4712–4727.

47. Yang, H., J. Yu, …, C. He. 2007. Interaction between single molecules of Mac-1 and ICAM-1 in living cells: an atomic force microscopy study. *Exp. Cell Res.* 313:3497–3504.

48. Williams, P. M. 2003. Analytical descriptions of dynamic force spectroscopy:behaviour of multiple connections. *Anal. Chim. Acta.* 479:107–115.